PHYSICAL REVIEW B, VOLUME 63, 121313(R)

Near-field imaging of one-dimensional excitons delocalized over mesoscopic distances

Andrea Crottini,[1] JL. Staehli,[1] Benoît Deveaud,[1] Xue-Lun Wang,[2,3] and Mutsuo Ogura[2,3]
[1]*Physics Department, Swiss Federal Institute of Technology Lausanne, CH-1015 Lausanne-EPFL, Switzerland*
[2]*Electrotechnical Laboratory, 1-1-4 Umezono, Tzukuba, Ibaraki 305-8568, Japan*
[3]*CREST-Japan Science and Technology Corporation (JST), Japan*
(Received 29 November 2000; published 13 March 2001)

Near-field optical spectroscopy is used to investigate the effects of disorder in the optical processes in semiconductor quantum wires. We observe photoluminescence emissions from extended, delocalized excitons at low temperatures (5 K) and low excitation densities. Combining high spectral and spatial resolution, we isolate homogeneous emission lines from excitons delocalized over distances up to 600 nm in the fundamental state. The energies of the emissions are consistent with different quantum spatial confinements along the wire axis. Unlike the photoluminescence originating from localized excitons, these emission lines show a high degree of polarization along the axis of the wire.

DOI: 10.1103/PhysRevB.63.121313 PACS number(s): 73.21.Hb, 78.67.Lt

Since the pioneering work of Anderson,[1] the relationship between disorder and localization in mesoscopic systems has been attracting considerable interest. The transition between localized and delocalized (extended) electronic states, as a function of disorder and energy, has been the subject of intense theoretical and experimental activity.[2,3] In this respect, one dimensional (1D) systems such as semiconducting quantum wires (QWRs) play a fundamental role, and the reason is at least twofold: from the theoretical point of view, the reduced dimensionality permits one to also resolve complex models yielding rigorous results,[4] and from the experimental one, the crystal growth of these structures has reached a remarkable quality level, leading to a rich variety of transport and optical properties.[5] Among them, the reported lasing from the quantum wire's fundamental state at low and room temperature,[6–8] concretely represent issues for device applications.

The Coulomb interaction between charged carriers is expected to play a crucial role due to the pathological features of the Coulomb potential in 1D: the assignment of the nature of carriers to Luttinger or to Fermi liquid in these systems is still a highly debated issue.[9,10] Direct insight into the disorder-induced localization can be obtained by studying the low-temperature optical excitations in QWRs. Excitons turn out to be excellent probes of the disorder effects, because of their outstanding property to be neutral. Unlike charged carriers, the Coulomb interaction between excitons vanishes at low densities. Within its lifetime, an exciton can be regarded as a probe sampling the effects of a disordered confining potential. The energy of the emitted light, due to electron-hole radiative recombination, is a direct measurement of the effects of these potential fluctuations.[11–13]

We have studied high-quality (QWRs) grown by flow rate modulation epitaxy (FME), an improved version of the organometallic chemical-vapor deposition technique. The flux of vapors is stopped several times during the growth, enhancing the quality of self-ordering growth processes and yielding extremely smooth interfaces. This fabrication process has been described in detail elsewhere.[14] Photolithography and chemical etching produce a V-grooved structure on a GaAs substrate with a period of 4 microns. The overgrown structure consists of a 3 mm GaAs well embedded in 50 nm $Al_{0.33}GaAs_{0.67}$ barriers. The wire is spontaneously formed at the bottom of the groove, due to a self-organized growth process:[15] the transmission electron microscope image in Fig. 1(a) shows the cross section of the wire and the typical ''V'' shape (the effective dimensions are 5×15 nm). A 2 microns thick AlGaAs cap layer is grown on top of this structure, and then attacked by mechanical lapping in order to flatten the surface of the sample. Artifacts in optical measurements, due to surface grating effects at the sample-air interface, are therefore avoided. Finally, the surface is

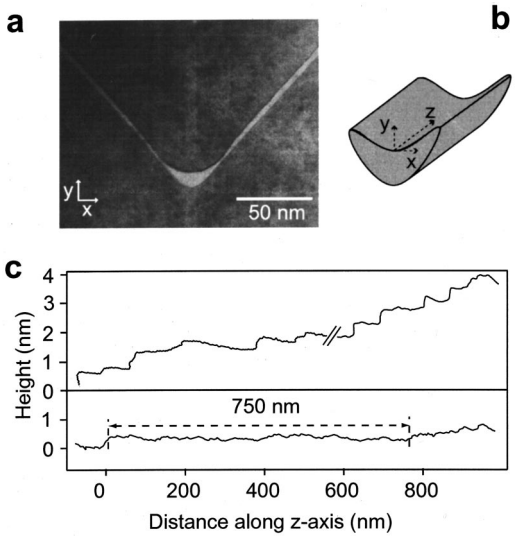

FIG. 1. (a) High-resolution TEM (transmission electron microscope) image of the QWR cross section taken along the crystal plane (01−1). (b) Shape of the confining potential experienced by excitons and definition of axis *xyz* referring to the wire. (c) AFM (atomic-force microscope) line scans at the growth interrupted wire-barrier interface, along the *z* line shown in (b) (crystal axis [01−1]). Monoatomic steps are found to delimit islands whose longitudinal dimensions range from 50 nm (upper scan) to about 700 nm (lower scan). The heights of these steps are about 0.4 nm, which is close to 0.3 nm, the nominal interatomic distance of GaAs along the [100] crystal axis [*y* in (b)].

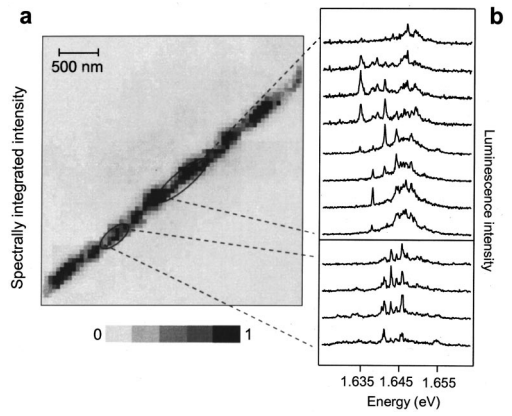

FIG. 2. (a) Intensity map obtained collecting the wire photoluminescence emission (laser excitation at 2.4 eV, power density 10 W/cm^2). (b) The photoluminescence from the wire is spectrally resolved and it shows a high number of spiky emission lines, originating from recombination of excitons localized in the structure (laser excitation at 2.4 eV with a power density of 0.01 W/cm^2). The spectra are collected at points 80 nm apart from each other along the wire axis.

chemically etched to have the GaAs wire at distances less than 100 nm below the surface. This is essential for high spatial resolution near-field measurements. Two-atomic-force microscope (AFM) scan profiles of a growth interrupted GaAs wire surface along a V groove are shown in Fig. 1(c). The AFM technique is able to resolve monolayer step variations in height and monoatomically flat zones are found over distances ranging from tens to hundreds nanometers. Of course at this level the AFM technique cannot give clear evidences of the absence of impurities and alloy fluctuations at the end of the fabrication process, after the AlGaAs barrier growth. Line scans in Fig. 1(c) show however that there are zones of more than 700 nm where no corrugation is present. This outstanding property is due to the highly efficient surface migration of group III species in the FME growth process.

The experimental set-up used in these measurements is a low temperature scanning near-field optical microscope (LT-SNOM). The validity of the SNOM technique in the study of the optical and transport properties of QWRs has been widely demonstrated.[16,17] In our case, the whole system operates in a He-flow optical cryostat and is kept at a temperature of 5 K. The sample is excited in far-field with the 2.41 eV line of an Ar^+ laser, the carriers are generated in the Al-Ga-As barrier and then trapped in the GaAs wire. The emitted photoluminescence is collected by the uncoated optical fiber of the LT-SNOM (collection mode), spectrally dispersed by a double monochromator and detected with a cooled CCD (charge-coupled device) camera, providing an ultimate spectral resolution of 0.08 meV. The advantage of using SNOM in collection mode is that optical images are not sensitive to carrier diffusion. The spatial resolution is 200 nm, as shown by the capability of the instrument to resolve different spectral emissions over such distances [Fig. 2(b)]. A typical combined spatial and spectral analysis of a QWR photoluminescence emission at 5 K is presented in Fig. 2. The map is obtained collecting the emission spectrally integrated over a window of 9 meV at the energy corresponding to the QWR excitonic line, as determined by far-field photoluminescence measurements (1.640 eV, FWHM 9 meV). We use laser power densities of the order of 10 and 0.01 W/cm^2 for emission maps and emission spectra, respectively; 1 h is usually needed to obtain an intensity map, and we acquire data over half an hour for a single emission spectrum.

The wire appears to be formed by a series of light emitting boxes aligned along the V-groove axis. The spectrally resolved emission shows several peaks with a full width at half maximum (FWHM) ranging from 0.8 (resolution limited) to 0.20 meV. The homogeneous spectral broadening, as can be derived from the excitonic lifetimes previously measured in our samples,[18] is estimated to be 0.01 meV. Larger linewidths, as in our case, can originate from fast dephasing times, electron-hole exchange interactions[18] or, as recently observed[19] in quantum dots, from charge-discharge effects with near impurities, which can produce Stark energy shifts on the excitonic emission, accounting for larger FWHMs in the time-integrated spectra. The linewidths do not depend either on excitation power densities or on the distance between the tip and the surface of the sample, excluding spectral diffusion effects and induced stress field effects.[20] The well-resolved peaks are due to emission from zero dimensional (0D) excitons localized in the GaAs AlGaAs QWRs inhomogeneities. These are quite common features in quantum wells[21] and wires.[22,23] We performed the spectral analysis of the emission over several zones of the sample and we found that the number of involved peaks is in the general between 4 and 20. Due to the extremely low excitation densities used here, the observed peaks are expected to originate from recombination of ground-state excitons, and not of excited states in the same dot. The intensity of the different peaks changes along the wire without any correlation: the intensity maxima of different lines are never found to be inside the same collection spot. This confirms a ground-state emission mechanism. Considering a collection spot size of 200 nm (FWHM), the localization length along the wire can be estimated to range between 10 and 50 nm, on average. This rough estimation could slightly change depending on the amount of spatial overlap or gaps between excitons.

In particular zones of the sample, we can isolate one single homogenous excitonic emission line (Fig. 3, 0.13 meV FWHM). These emissions can be observed over distances up to 600 nm, i.e., three times the spatial resolution of our system, and can be considered to originate from truly 1D quasidelocalized states. These distances are longer than any other length scale involved here. In particular, these mesoscopic distances are a hundred times the Bohr radius ($\sim$5–10 nm) of excitons in GaAs-based semiconducting heterostructures. To the best of our knowledge, up to now the presence of delocalized excitons in low-dimensional semiconductors at low temperatures and densities has only been inferred from measurements of light absorption, photoluminescence excitation,[24] four-wave mixing techniques, and resonant Rayleigh scattering.[3] These states have therefore been found in experiments where they were involved in a resonant ab-

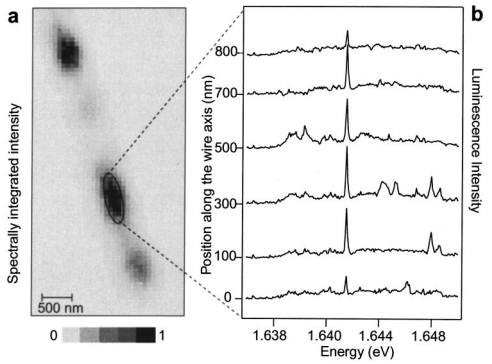

FIG. 3. (a) The spectrally resolved emission form the wire-elongated box (circle in a) reveals the presence of a single homogeneous (0.13 meV FWHM) emission line delocalized over 600 nm (b). The laser excitation for the map and the spectra is as in Fig. 2.

sorption process, but not in a spontaneous recombination process. In a nonresonant photoluminescence experiment and low excitation density regime, electron-hole pairs excited by light relax to localized states before they recombine radiatively. This usually prevents one from observing spontaneous emission from delocalized states. Here we give clear evidence that some samples feature a high enough quality to allow for the radiative recombination of delocalized excitons. In our case, in contrast to Ref. 24, where an extended state is inferred from the presence in absorption of an ubiquitous excited state, delocalization is revealed by the emission from a ground-state exciton.

We now address the question why in certain areas of the sample such delocalized states are present, and localized states are missing. In our samples, three types of disorder-induced localization should be considered. First, fluctuations of the confining potential, due to long-range corrugation effects at interfaces, can occur in the sample on length scales that are comparable to the ''macroscopic'' distances mentioned above. This is corroborated by our AFM data [Fig. 1(c)]. Second, alloy variations at the wire-barrier interface, due to a random distribution of Ga and Al atoms, can happen on an atomic scale without giving rise to segregation and coalescencence on a longer scale. This results in a rapidly varying confining potential, which is averaged by the excitation wave function and prevents localization.[13] Third, the presence of randomly distributed impurities, with concentration as low as 10^5 cm^{-1} as in this sample, is expected to give Anderson localization lengths for electrons larger than several microns in QWRs.[25] The interaction between these impurities and excitons should play an even smaller role, due to the neutrality of these particles. It is therefore clear that, if realistic disorder phenomena are taken into account, the physical quantity that determines the localization lengths in these systems is the long-range corrugation. As a consequence, the zones where monoatomically flat interfaces are present over several hundreds of nanometers represent an ideal two-dimensional confinement for electrons and holes. The center of mass of the exciton is free to move along the wire, experiencing a constant mean potential over distances which are a hundred times its wave-function size: thus it can be considered to be genuine 1D exciton.

In Figs. 4(a) and 4(b) the spatial transition from 1D extended to 0D localized states is shown. From the emission spectra, collected along the wire at points 100 nm apart from each other, it is clearly seen that in two subsequent zones, labeled A and B, the emission originates from 1D excitons which extend over distances of 400 and 200 nm (resolution limited), respectively. The energy difference between the two emission lines may be understood very schematically in the following way. We calculated the electronic energy levels for electrons and holes, in the envelope function framework.[13] Any variation of the shape of the confining potential in the *xy* plane [Fig. 1(b)], i.e., a change of one monolayer in the cross-section dimensions of the wire gives an energy shift of more than 10 meV. As a consequence, this energy separation is due to a different confirming potential

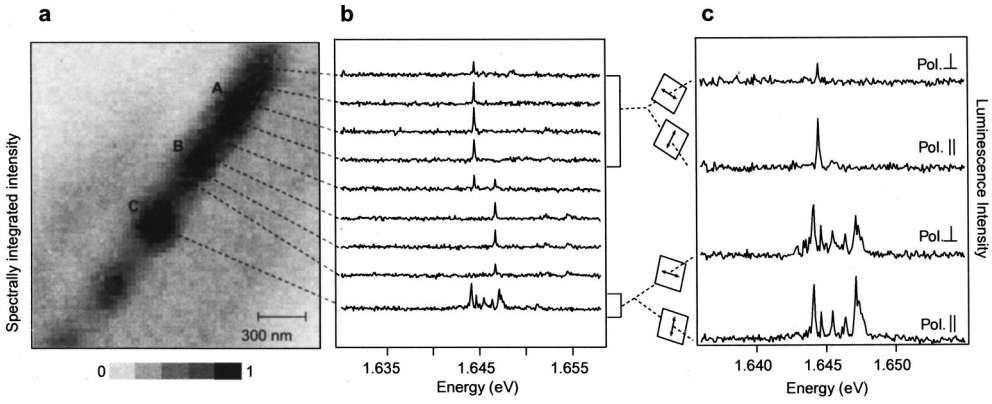

FIG. 4. (a), (b) The spectra corresponding to the zones A and B are collected at points 100 nm apart from each other. The presence of two peaks between A and B is due to the optical resolution of our LT-SNOM: at that point, the emissions from both zones are collected. The different dimension of the confining potential along the wire axis can account for the observed energy separation between the two emission lines from A to B. The emissions from the dotlike region C correspond to excitons localized in the structure. (c) Using a linear-polarization filter, we determine the polarization components of the emission (from zones A and C in a) parallel (Pol.$\|$) and perpendicular (Pol.$\perp$) to the wire axis. The emission from 1D delocalized excitons (zone A) is found to be strongly polarized parallel to the wire, while no anisotropy is observed for the 0D excitons (zone c).

experienced by electrons and holes along the axis of the wire [z in Fig. 1(b)]. The computed energy level difference between a 400 nm long and a 60 nm long wire is 2.1 meV and can account for the observed separation. The zones A and B therefore can be considered to be wirelike boxes, each of them having the same cross-sectional shape, but different lengths—the actual length of B is eventually overvalued to 200 nm, the limit of our optical resolution. In the following zone, labeled C, the spectrum consists of multiple peaks, demonstrating the presence of excitons confined in dots aligned along the wire. The number of peaks and their intensity ratio do not change if the excitation density is lowered, confirming that the observed lines are not due to different excitonic states in the same dot.

The spectra in Fig. 4(c) are clear fingerprints of the different natures of the optical transitions in the wirelike and the dotlike confining potential. Here we check the polarization degree of the photoluminescence signal collected by the fiber. In order to determine the polarization component of the emitted light along the wire axis, we illuminate the surface of the sample with a laser beam, linearly polarized along the wire axis. The reflected light is collected by the same fiber and its polarization vector at the fiber output is used as a reference, giving the direction corresponding to the wire axis. Using a linear-polarization filter, we found that the emissions from zones A and B show an extremely high degree of linear polarization along the wire axis. We define the degree of polarization as $P=(I_{\parallel}-I_{\perp})/(I_{\parallel}+I_{\perp})$, where $I_{\parallel}$ and $I_{\perp}$ are the intensities of the two components of the signal, collected with the axis of the analyzer parallel or perpendicular to the wire axis, respectively. The experimental value of P corresponding to the emission of the wirelike zones is 0.8 ± 0.1, indicating a strong polarization parallel to the wire, while no polarization anisotropy is observed in the emission from the dotlike region (zone C). From the theoretical point of view, the two-dimensional confinement and the consequent valence-band mixing at the center of the Brillouin zone can account for the polarization anisotropy in quantum wires.[26,27] We emphasize that strain-induced polarization anisotropy effects can be excluded due to the absence of wire-barrier lattice mismatch. Localization effects tend usually to mask this anisotropy, changing the exciton wave function and the related symmetry from 1D to 0D-like.[28] With respect to the polarization state of the emitted light, by means of high spatial resolution measurements, we can unambiguously associate the anisotropy and the isotropy to the emissions from 1D excitons and from 0D excitons, respectively. This highlights the intrinsically different nature of optical recombinations from extended and localized electron-hole pairs.

In conclusion, we have observed photoluminescence emissions from delocalized excitons in quantum wires. We report delocalization lengths up to 600 nm and strong polarization anisotropy along the wire axis in emission. These excitons, unaffected by disorder, represent therefore an ideal laboratory to study further the expected unusual characteristics of interacting 1D Fermi systems.

We are indebted to F. Lelarge, D. Y. Oberli, C. Ciuti, M. Saba, V. Ciulin, G. R. Hayes, and M.-A. Dupertuis for stimulating discussions. We are also grateful to P. W. Anderson and A. Baldereschi for clarifying discussion. A.C. acknowledges financial support by Fonds National Suisse de la Recherche Scientifique.

[1] P. W. Anderson, Phys. Rev. **109**, 1492 (1958).
[2] N. F. Mott and E. A. Davis, *Electronic Processes in Noncrystalline Materials* (Oxford University Press, New York, 1979).
[3] J. Hegarty and M. D. Sturge, J. Opt. Soc. Am. B **2**, 1143 (1985).
[4] B. Kramer and A. MacKinnon, Rep. Prog. Phys. **56**, 1469 (1993).
[5] M. J. Kelly, *Low Dimensional Semiconductors* (Oxford Science Publications, Oxford, 1995).
[6] W. Wegscheider *et al.*, Phys. Rev. Lett. **71**, 4071 (1993).
[7] L. Sirigu, Phys. Rev. B **61**, 10 575 (2000).
[8] T. G. Kim *et al.*, Physica E **7**, 508 (2000).
[9] M. Rother *et al.*, Physica E **6**, 551 (2000).
[10] B. Yu-KuangHu and S. D. Sarma, Phys. Rev. Lett. **68**, 1750 (1992).
[11] C. Weisbuch *et al.*, Solid State Commun. **38**, 709 (1981).
[12] U. Jahn *et al.*, Phys. Rev. B **54**, 2733 (1996).
[13] G. Bastard, *Wave Mechanics Applied to Semiconductor Heterostructures* (Les Editions de Physique, Paris, 1988).
[14] X. L. Wang, M. Ogura, and H. Matsuhata, Appl. Phys. Lett. **66**, 1506 (1995).
[15] G. Biasiol and E. Kapon, Phys. Rev. Lett. **81**, 2962 (1998).
[16] T. D. Harris *et al.*, Appl. Phys. Lett. **68**, 988 (1996).
[17] A. Richter *et al.*, Phys. Rev. Lett. **79**, 2145 (1997).
[18] J. Bellessa *et al.*, Phys. Rev. B **58**, 9933 (1998).
[19] A. Hartmann *et al.*, Phys. Rev. Lett. **84**, 5648 (2000).
[20] H. D. Robinson and B. B. Goldberg, Phys. Rev. B **61**, R5086 (2000).
[21] K. Brunner *et al.*, Appl. Phys. Lett. **64**, 3320 (1994).
[22] J. Hasen *et al.*, Nature (London) **390**, 54 (1997).
[23] W. R. Tribe *et al.*, Appl. Phys. Lett. **73**, 3420 (1998).
[24] W. Qiang *et al.*, Phys. Rev. Lett. **83**, 2652 (1999).
[25] L. Dongzi and S. Das Sarma, Phys. Rev. B **51**, 13 821 (1995).
[26] C. R. McIntyre and L. J. Sham, Phys. Rev. B **45**, 9443 (1992).
[27] P. Ils *et al.*, Phys. Rev. B **51**, 4272 (1995).
[28] F. Vouilloz *et al.*, Phys. Rev. B **57**, 12 378 (1998).